Pergamon

Int. J. Heat Mass Transfer. Vol. 39, No. 8, pp. 1719–1727, 1996

0017-9310/96 $15.00 + 0.00

0017-9310(95)00199-9

Heat transfer enhancement in a converging passage with discrete ribs

ZHENGJUN HU and JIARUI SHEN

Institute of Engineering Thermophysics, Chinese Academy of Sciences, Beijing 100080, People's Republic of China

(*Received* 15 *April* 1955)

Abstract—An experimental investigation has been carried out to measure detailed distributions of internal heat transfer coefficients in a model of a blade mid-chord convergent cooling passage. The test is performed with a staggered array of 45° discrete ribs, and also with a combination of the discrete ribs with grooves on two opposite walls of the passage for a range of engine representative Reynolds numbers from 1.0×10^4 to 5.0×10^4. The data is presented as contours of enhancement factors (defined as heat transfer coefficient divided by heat transfer coefficient in the absence of the discrete ribs). The data of stream-wise Nusselt number are correlated. The area-averaged enhancement factors of 3 to 4 and 2.5 to 3.2 are obtained, respectively, for both promoter configurations studied. The flow visualization has been performed. The complex flow patterns observed successfully provide a mechanismic explanation for the contours of enhancement factors. The friction factors are also measured in the passages with the discrete ribs and combination of the discrete ribs with grooves.

INTRODUCTION

In a gas turbine blade cooling design, repeated rib-turbulators are usually cast on the opposite walls of the internal cooling passages in order to enhance the removal of heat from the blade external surfaces. The effects were investigated extensively of rib geometry (such as rib height, rib width, spacing, angle of attack, etc.) and flow Reynolds number on the heat transfer and friction loss in the fully developed region of ribbed passages [1–10].

The emphasis of these previous works was placed on the full transverse ribs (ribs that stretch across the width of the passage with any angle of attack). The investigations indicated that air flow over transverse ribs with angles of attack of 90° separates at a distance of about one rib width from the rib edge. The flow reattachment usually occurs at the mid-way between the ribs. High heat transfer occurs in the vicinity of the reattachment location. The typical value of the area-averaged heat transfer enhancement factor is about two or less for the full transverse ribs. In the case of full oblique ribs (angles of attack $\neq 90°$), there is a secondary flow in a direction paralleled to the rib axis [6–10]. The interaction between the main flow and the secondary flow results in the vigorous mixing of the air flow near the rib and wall, and further enhances the heat transfer to the air flow. There is, however, little data concerned with the enhancement of internal heat transfer coefficient as air flow passes through a passage with discrete ribs on two opposite walls [11–13]. It is evident that a need exists for demonstration of the effects of replacing the full ribs by short segments of the full ribs on the heat transfer and friction. It is not doubtful that the detailed measurements of local heat transfer coefficients and observation of complex flow patterns on the wall with inclined discrete ribs will be of great importance.

In this paper, two different test sections have been investigated for a range of engine representative Reynolds numbers from 1.0×10^4 to 5.0×10^4. Firstly, a staggered array of 45° discrete ribs on two opposite walls of a square passage was tested. Secondly, a combination of the discrete ribs with discrete grooves in alternate rows of ribs and grooves was tested. Both of the test sections have the same geometric parameters and arrangement.

Detailed distributions of local heat transfer coefficients have been obtained in the passages studied. The measurement for flow friction has been performed. The complex secondary flow on the ribbed wall has been observed. The area-averaged heat transfer coefficients, which have been achieved in the passages studied in the work, are approximately double the heat transfer coefficients obtainable with full transverse ribs.

It is hoped that the detailed local and area-averaged heat transfer data presented in this paper will be used in blade cooling design methods.

EXPERIMENTAL APPARATUS AND METHODS

A schematic diagram of the experimental apparatus is shown in Fig. 1. The air from the compressor passes through the cleaner, orifices, stabilizer and transition duct, enters the test section, and finally flows out through the exit duct. The test section is a 7.5 times engine-size model of a blade mid-chord cooling pass-

NOMENCLATURE

A	heat transfer surface area
C_p	specific heat at constant pressure
e	rib height
e'	groove depth
EF	enhancement factor
EF	area-averaged enhancement factor
f_r	friction factor in rib-roughened converging square passage
f_s	friction factor in smooth square passage
$\bar{f}_s$	friction factor in smooth converging square passage
De	passage hydraulic diameter
G	mass flow rate
$\dot{G}$	mass flux
$h_{(x,y)}$	local heat transfer coefficient
L	length of test section
Nu_x	local Nusselt number
ΔP	pressure drop in the test section
q	heat flux
Q	heat flow rate
Pr	Prandtl number
P	rib pitch
Re	Reynolds number
S	length of discrete rib
S'	space length between two discrete ribs
St	Stanton number
T_f	air temperature
T_w	wall temperature
V_x	average velocity on a cross-section of the passage
W	rib width
W'	groove width.

Greek symbols

ρ	air density
μ	average viscosity of air.

Subscripts

x	local value at coordinate x
r	value in passage with rib-roughened walls
s	value in passage with smooth walls.

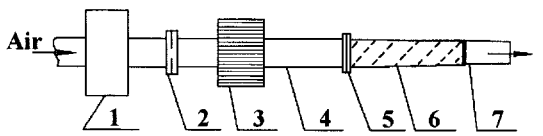

1–Cleaner 2–Orifices 3–Stabilizer 4–Transition Duct 5–Flange 6–Test Section 7–Exit Duct

Fig. 1. A schematic diagram of the apparatus.

age. This duct is 233 mm long and has been idealized, in that it has a square section which decreases from an entry of cross-sectional dimensions 38 mm by 38 mm to an exit of cross-section dimensions 32 mm by 32 mm. The actual engine passage has rounded corners, but it was judged that this simplification to the geometry would have little influence on the applicability of the heat transfer data.

The tested two opposite walls with a staggered array of 45° discrete ribs were made of stainless steal and the other two opposite walls with smooth interior surfaces were made of thermal insulation material. The rib array on each wall is a mirror image of that on the other (that is, corresponding ribs on the two opposite walls are paralleled and aligned). The typical geometric parameters of the test section are shown in Fig. 2. In the case of combination of the discrete ribs with grooves, the geometry of the test section is exactly the same as that in Fig. 2 but the rows of discrete ribs were replaced by the rows of discrete ribs and discrete grooves. The discrete ribs and grooves were, in turn, arranged in flow direction, they have the same dimensions and position as the rows of discrete ribs only. The two ribbed walls had equal and uniform heat flux which were heated by electrical heaters. 100 thermocouples, 0.2 mm diameter, were welded on an area of interest of the test walls ($x/L = 0.5 \sim 0.8$), and 10 thermocouples were uniformly laid on the centerline of a tested wall along the flow direction for the longitudinal wall temperature measurement. Inlet and outlet air flow temperatures were also measured by thermocouples. Static pressure taps were located at entry and exit of the test section, respectively, for pressure drop measurements. The air supply to the experimental apparatus was variable giving a range of Reynolds numbers of 1.0×10^4 to 5.0×10^4 based on the hydraulic diameter De and flow velocity V, the local heat transfer coefficients $h_{x,y}$ would be obtained as follows:

$$h_{x,y} = \frac{Q}{A(T_{w_{x,y}} - T_{f_x})} = \frac{q}{T_{w_{x,y}} - T_{f_x}}. \quad (1)$$

Since the aim of the work was to quantify the enhancement to the internal heat transfer coefficients in the blade passage brought about the discrete ribs, the data is presented as contours of enhancement factors EF. All of the enhancement factors presented were obtained by normalizing the local heat transfer coefficients measured by that along the centerline of the passage in the absence of the ribs. Heat transfer coefficients in the passage without ribs were calculated using the following equation given in Kays [14]

$$St_x Pr^{0.4} = 0.0295 Re_x^{-0.2} \quad (2)$$

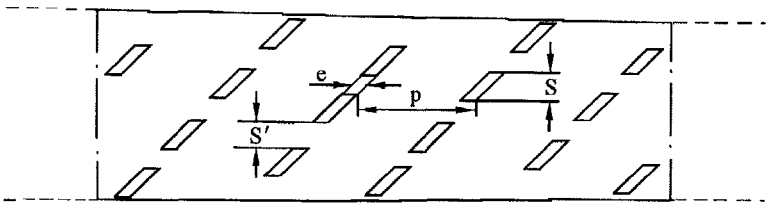

e/De=0.0625 P/e=9 S/e=2.5 S/S′=1
(W=e=2mm W′=e′=2mm)

Fig. 2. Typical geometric parameters of the tested wall.

where Reynolds number and Stanton number defined as, respectively,

$$Re_x = \int_0^x \frac{\rho V_x}{\mu} dx$$

$$St_x = \frac{h_x}{\rho V_x C_p}.$$

Averaged velocity on a cross section of the passage, V_x, is a function of longitudinal coordinate x only, and

$$V_x = \frac{G}{\rho De_x^2}.$$

The flow friction loss through the passage was measured under isothermal conditions and the friction factor was obtained from the following equation:

$$\bar{f}_r = \frac{\Delta P}{4(L/De)(\dot{G}^2/2\rho)}. \quad (3)$$

The friction factor in a square-nonconverging passage without ribs was calculated using the Karman–Prandtl equation [6]

$$\frac{1}{\sqrt{f_s}} = 4.0 \log_{10}(Re\sqrt{f_s}) - 0.40 \quad (4)$$

which was inferred into equation (5) for the square-converging passage without ribs

$$\bar{f}_s = \frac{De^5}{L} \int_0^L \frac{f_{s_x}}{De_x^5} dx. \quad (5)$$

RESULTS AND DISCUSSIONS

To clearly examine how the heat transfer in the square converging passage is affected when full ribs on two opposite walls of the passage are replaced by the discrete ribs and the combination of the discrete ribs with grooves, only the contours of the enhancement factors in the region of interest, $x/L = 0.5 \sim 0.80$, on the rib-roughened wall are presented here. For the development of heat transfer correlations, the data of streamwise heat transfer coefficients is given in Nusselt numbers.

Heat transfer measurement in the passage with discrete ribs

The contours of heat transfer enhancement factors in the passage with the discrete ribs are plotted in Fig. 3. An overall examination of the figure reveals similar contours for different Reynolds numbers. All of the contours are basically symmetrical about the alignment of the ribs. The lines of the contours at the front of and behind the ribs are basically parallel to the ribs. For a particular rib, practically larger enhancement factors occur in the regions immediately upstream and downstream of the rib, respectively, also in the regions between the two opposite ends of the ribs (where a corresponding segment of a full rib is cut off). The smaller enhancement factors take place in the further upstream region of the rib, and the position (where smaller enhancement factors take place) moves towards the leading edges of the ribs along the spanwise row of the ribs. The enhancement factors in the region downstream of the rib tend toward a gradual decrease in flow direction.

In addition, compared to enhancement factors in the region near the bottom wall where the angle between the rib and main flow direction is 45°, the enhancement factors are somewhat small in the region near the top wall where the angle between the rib and main flow direction is 135°.

It is of interest to note that, different from the full rib case, the weak heat transfer behind the ribs and in the corner regions of the passage is considerably improved, since the full ribs were replaced by the discrete ribs. The level of heat transfer coefficients on the ribbed wall tends to be uniform.

The distribution of the enhancement factors could be explained by flow separation at the discrete rib, reattachment on the wall, and complex recirculation created by periodically discrete ribs. In fact, the complex flow field and secondary flow have been observed (such as secondary flow front rib and behind rib

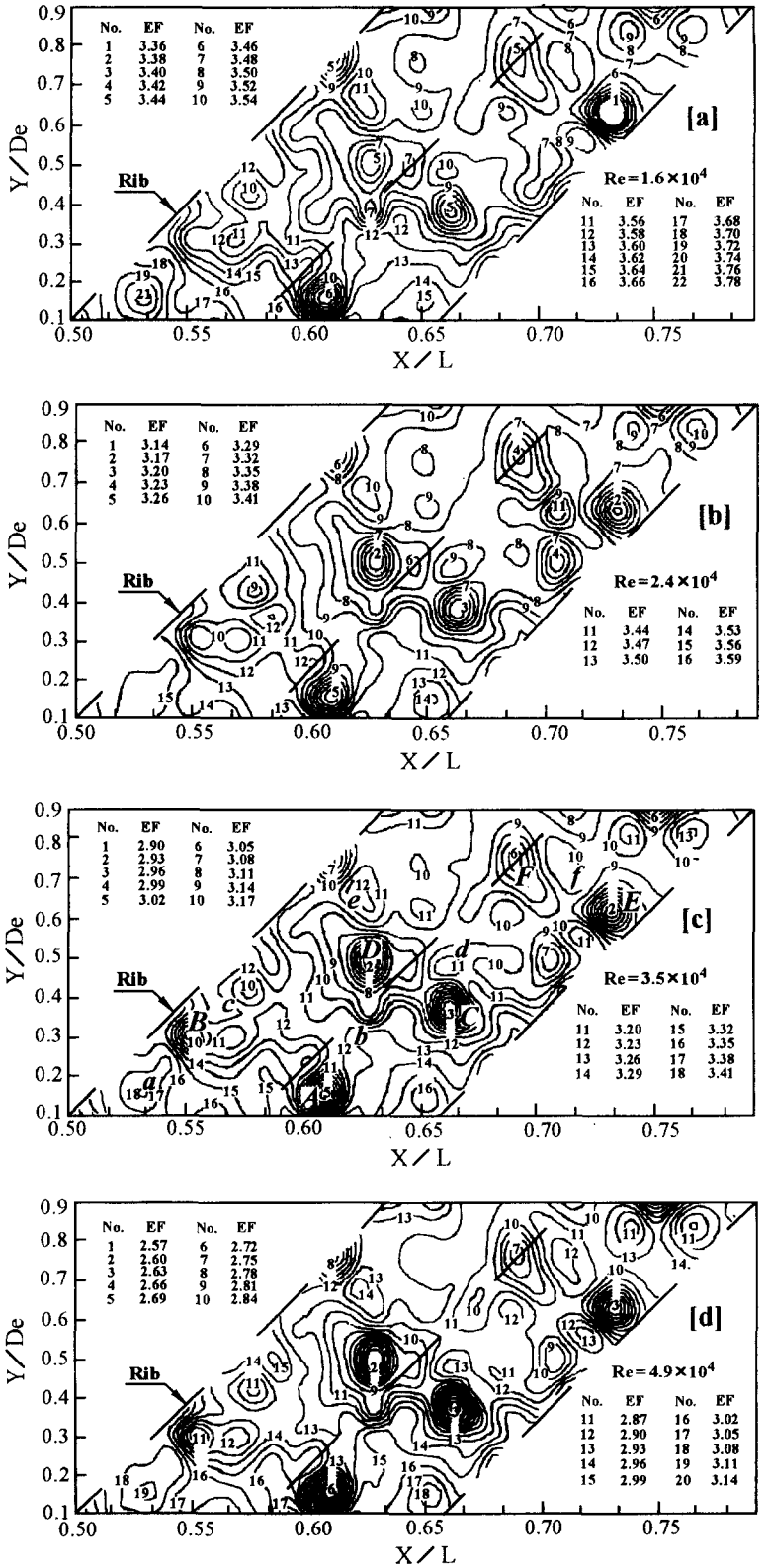

Fig. 3. Contours of enhancement factors for discrete ribs.

caused by the orientation of the ribs, secondary flow resulting from separation on the end edges of the discrete ribs, and longitudinal swirling flow over the ribs, etc.) by means of visualization performed in this study. The vigorous mixing of the flowing air near the wall and ribs greatly enhances the heat transfer to the air flow.

Heat transfer measurement in the passage with combination of the discrete ribs with grooves

The contours of enhancement factors are shown in Fig. 4 for a combination of the discrete ribs with grooves. The contours behave in a similar way for different Reynolds numbers. The contours are, however, significantly different to those in the case of the discrete ribs only. It is found from Fig. 4 that lower enhancement factors occur in the regions immediately upstream and downstream of the grooves, although higher enhancement factors still take place in the regions immediately upstream and downstream of the discrete ribs. It would seem that velocity of air flow is low near the bottom of the groove, and disturbance caused by the grooves is not strong enough to promote heat transfer in the region near the grooves. Compared to the discrete rib case, distribution of enhancement factors becomes more uniform, although the difference between the values of enhancement factors in both regions near the bottom and top walls becomes larger.

Streamwise Nusselt numbers

The streamwise Nusselt numbers on the centerline of the roughened wall studied are plotted in Figs. 5 and 6, respectively, as a function of nondimensional axial coordinate, x/De, for both cases of the discrete ribs and combination of the discrete ribs with grooves. The streamwise Nusselt numbers presented here are based on the area-averaged heat transfer coefficients and hydraulic diameter, De, of the passage. The decrease in Nusselt numbers along the flow direction in the entrance region of the passage, as shown as Figs. 5 and 6, could be considered as the entrance effect, where thermal boundary layer and the turbulence induced by the discrete ribs or the combination of the discrete ribs with grooves has not yet been fully developed, although flow has fully developed already. The increase in Nusselt numbers towards the passage exit is due to the flow acceleration as the passage converges. Inspection of Figs. 5 and 6 indicates that in the discrete rib case, the turning location from decrease to increase in Nusselt number takes place earlier than that in the case of the combination of the discrete ribs with grooves. This suggests that the discrete ribs could strongly disturb flow, and therefore promote greater heat transfer than the combination of the discrete ribs with grooves.

It is clear that Nusselt numbers increase with increasing Reynolds numbers for both promoter configurations.

Correlations of heat transfer data can be presented in the following, with deviations of $\pm 5\%$

$$Nu_x\, Re^{-n} = a\left(\frac{x}{De}\right)^2 + b\left(\frac{x}{De}\right) + c. \qquad (6)$$

The coefficients of equation (6) are given in Table 1

Area-averaged enhancement factors

The area-averaged enhancement factors are shown in Fig. 7 for both promoters studied. It is obvious that the area-averaged enhancement factors decrease as flow Reynolds number increases for both cases. The level of the area-averaged enhancement factors is about 3–4 for the discrete ribs, and 2.5–3.2 for combination of the discrete ribs with grooves, respectively, for the range of Reynolds numbers from 1.0×10^4 to 5.0×10^4.

Flow visualization results

Figure 8 shows qualitative flow patterns around a discrete rib with an angle of attack of 45°. The sketch, Fig. 9, is based on collective evidence from streamline patterns visualized on the surface with the discrete rib. It can be seen from these figures that the streamlines are curved near the leading face of the rib where the boundary layer is skewed [15]. A flow separation is found in the close vicinity of the leading edge of the rib. A recirculation zone is observed adjacent to the leading face of the rib, shown as the light color zone in Fig. 8a. The separation is also found near the end face of the rib. It can clearly be seen from Fig. 8c that a secondary flow front rib is moving in helical vortices along the rib orientation, and is passing through the space between the two end faces of the ribs. It is understandable that the occurrence of secondary flow front rib is due to interation of the recirculating flow created by separation from the leading edge of the rib with the moving flow along the rib axis caused by separation at the end face of the rib. It is true that as a result of the secondary flow front rib, the lines of contours of enhancement factors immediately upstream of the discrete rib, as shown in Fig. 3, behave parallel to the rib. It is reasonable to say that the secondary flow front rib would greatly promote the heat transfer to fluid in the region immediately upstream of the rib.

It can also be seen from Fig. 8 that there is a stream of secondary flow behind the rib. This is because a negative pressure gradient along the orientation of the rib exists behind the rib. Higher values of enhancement factors in the immediately downstream of the rib could be explained by scouring of the secondary flow behind rib.

It is of interest to note that flowing longitudinal vortices resulted from interaction of the secondary flow behind the rib, with the flow over the top face of the rib swingingly moving towards the direction deviated from the main flow. It could be expected that the

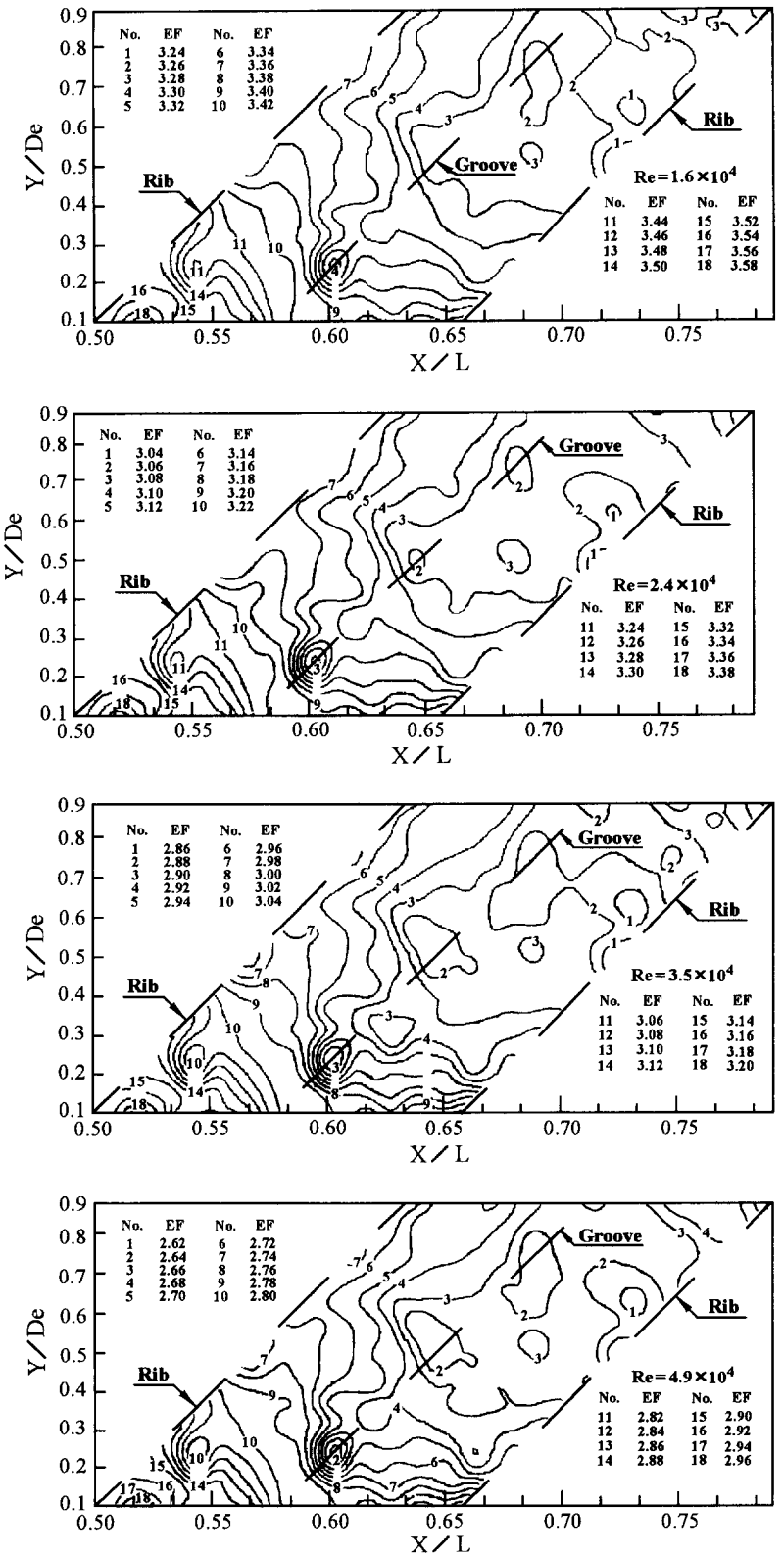

Fig. 4. Contours of enhancement factors for combination of discrete ribs with grooves.

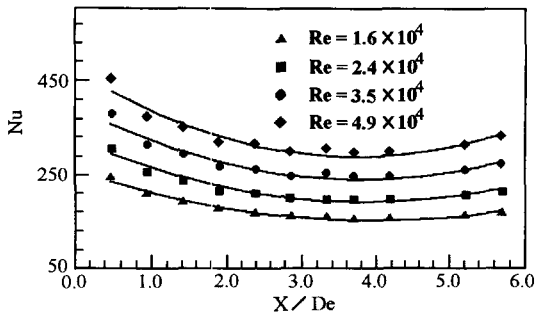

Fig. 5. Distributions of streamwise Nusselt numbers for discrete ribs.

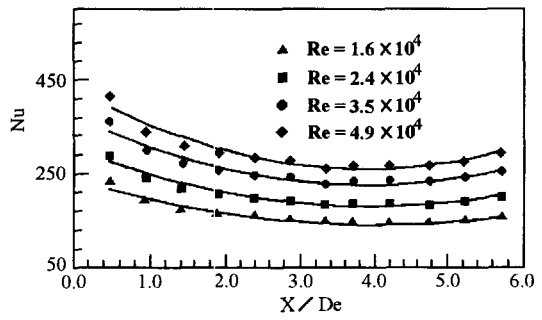

Fig. 6. Distributions of streamwise Nusselt numbers for combination of discrete ribs with grooves.

Table 1. Coefficients in correlation (6)

Promoter	n	a	b	c
Discrete ribs	0.55	0.035	−0.261	1.262
Combination of discrete ribs with grooves	0.60	0.019	−0.146	0.710

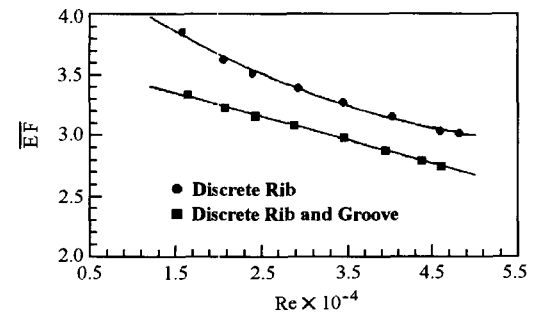

Fig. 7. Variation of area-averaged enhancement factors with Reynolds numbers.

stronger the secondary flow behind rib, the larger the angle of longitudinal vortex flow deviated from the main flow direction. Perhaps, a contribution of the longitudinal vortices to heat transfer is the local peak value of the enhancement factors in the region between the end faces of the ribs (see, mark a, b, c, d, e, f in Fig. 3c). It could be judged that these places are certainly reattachment positions of the flowing longitudinal vortices. The smaller value of the enhancement factors in the region of upstream of the rib (see, mark A, B, C, D, E, F in Fig. 3c) could be attributed to the stopping of the development of three-dimensional flow boundary layer between end faces of the ribs, because of the disturbance of the longitudinal vortices.

The flow field observed near the wall with the discrete rib is shown in Fig. 10. Inspection of Fig. 10 shows that there is a reverse flow in the region near the top wall, since there is obstruction of the passage top wall to the secondary flow moving along the rib orientation. As a result of the reverse flow, the secondary flow behind the rib and flowing longitudinal vortices is progressively weakened near the top wall. There is a consequent decrease in the enhancement factors (see, mark F in Fig. 3a). This is just like the case of full transverse ribs, the low enhancement factors occurring in the vicinity of the rib.

Flow friction measurement

Flow friction measurement results are shown in Fig. 11 as $\bar{f}_r/\bar{f}_s$. It can be seen that the level of $\bar{f}_r/\bar{f}_s$ increases as the Reynolds number decreases for both cases studied. Compared to the corresponding smooth passage, friction factors increase by a factor of about nine. In the discrete rib case, friction factors are about 20% higher than that in the case of a combination of the discrete ribs with grooves for a range of Reynolds numbers from 1.0×10^4 to 5.0×10^4.

CONCLUSION

Detailed maps of enhancement factors have been produced in a converging passage, with the discrete ribs and combination of the discrete ribs with grooves. Flow visualization has been performed to indicate complex flow patterns and to understand the effect of secondary flow induced by the discrete ribs on heat transfer enhancement. Several streams of secondary flow (such as secondary flow front rib, secondary flow behind rib, longitudinal vortex flow, etc.) have been found. The contours of the enhancement factors obtained are in very good agreement with the complex flow patterns visualized on the surface with the discrete ribs. Flow friction measurement has been carried out. The findings of the work include the following:

(1) The replacement of full ribs by the discrete ribs and combination of the discrete ribs with grooves results in a high value of heat transfer enhancement factors. Heat transfer characteristic and augmentation could be attribute to secondary flow resulting from the inclined discrete ribs and vigorous mixing of secondary flow with main flow.

(2) The area-averaged enhancement factors of 3–4 for the discrete ribs and of 2.5–3.2 for the combination of the discrete ribs with grooves have been obtained.

(3) The data of streamwise Nusselt numbers have been correlated with the deviation of $\pm 5\%$.

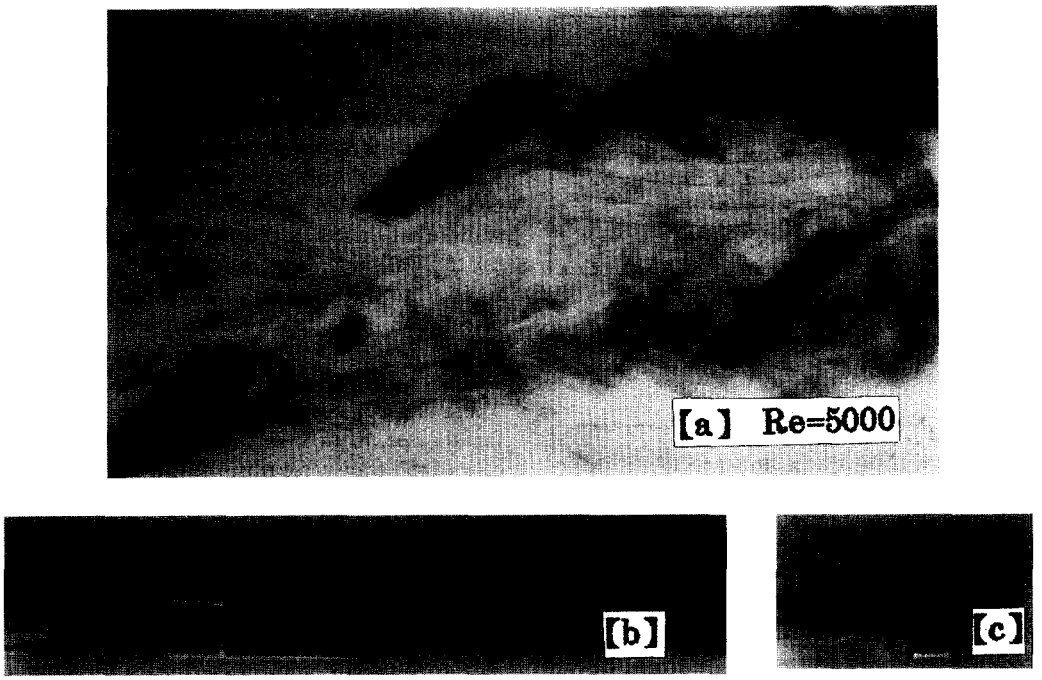

Fig. 8. Flow patterns near to the wall with discrete ribs: (a) vertical view, (b) lateral view ($Re = 7000$), (c) vortices front rib ($Re = 7000$).

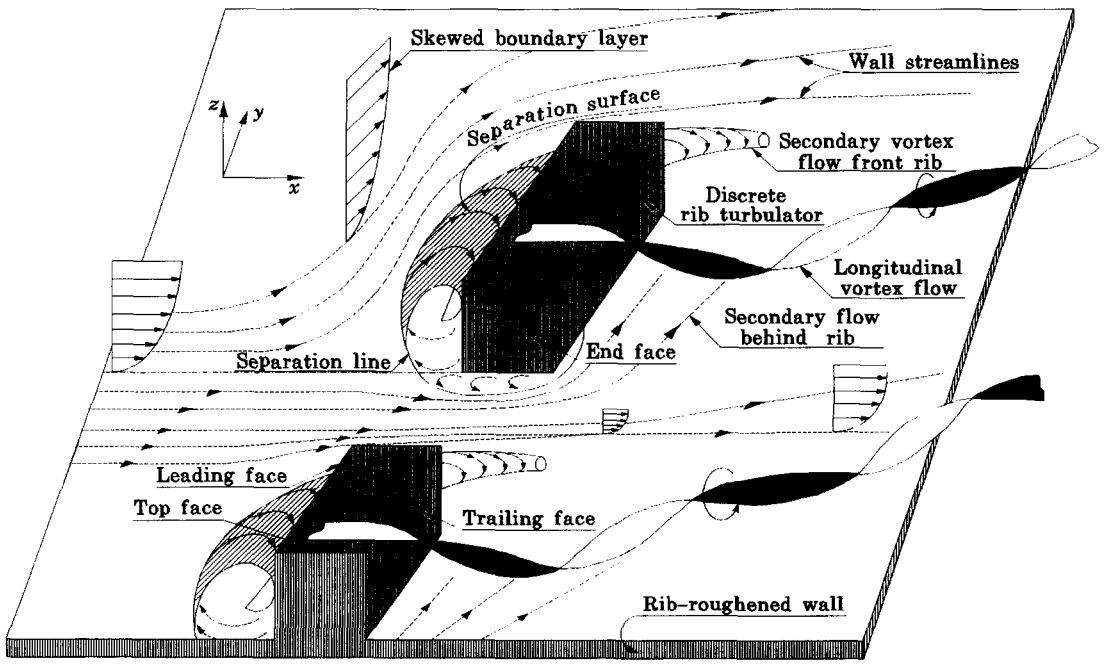

Fig. 9. Interpretation of the flow structures near to the wall with discrete ribs.

Fig. 10. Flow field near to the wall with discrete ribs.

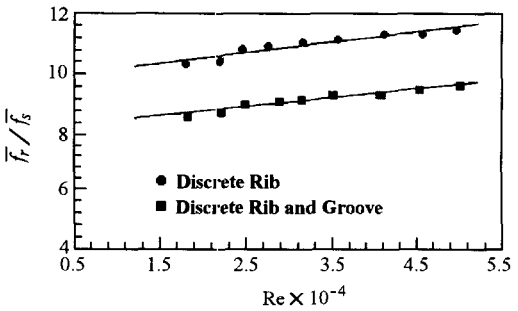

Fig. 11. Variation of $\bar{f}_r/\bar{f}_s$ with Reynolds number.

(4) The friction factors increase by a factor of about nine compared to the corresponding smooth passage for both the discrete ribs and combination of the discrete ribs with grooves. In the discrete rib case, friction factors are about 20% higher than in the case of the combination of the discrete ribs with grooves.

REFERENCES

1. F. Burggraf, Experimental heat transfer and pressure drop with two-dimensional turbulence promoter applied to two opposite walls of a square tube. In: *Augmentation of Convective Heat and Mass Transfer* (Edited by A. E. Bergles and R. L. Webb), pp. 70–79. ASME, New York (1970).
2. F. C. Yeh and F. S. Stepka, Review and status of heat-transfer technology for internal passages of air-cooled turbine blades, NASA Technical Paper 2232 (1984).
3. J. R. Shen, P. T. Ireland, Z. Wang and T. V. Jones, Heat transfer enhancement in a model of a blade cooling passage using combination of ribs and rib-grooves with film cooling holes, *Proceedings of the 6th International Symposium on Transport Phenomena in Thermal Engineering*, Seoul, Vol. 2, pp. 433–438 (1993).
4. J. R. Shen, Z. Wang, P. T. Ireland and T. V. Jones, Heat transfer enhancement within a turbine blade cooling passage using ribs with film cooling holes, 94-GT-232 (1994).
5. T.-M. Liou and J.-J. Hwang, Turbulent heat transfer augmentation and friction in periodic fully developed channel flows, *ASME J. Heat Transfer* **114,** 56–64 (1992).
6. J. C. Han, Heat transfer and friction in channel with two opposite rib-roughened walls, *ASME J. Heat Transfer* **106,** 774–781 (1984).
7. J. C. Han, J. S. Park and C. K. Lei, Heat transfer and enhancement in channels with turbulence promoters, *ASME J. Heat Transfer* **106,** 774–781 (1985).
8. J. C. Han and J. S. Park, Developing heat transfer in rectangular channels with rib turbulators, *Int. J. Heat Mass Transfer* **31,** 183–195 (1988).
9. J. C. Han, Heat transfer and friction characteristics in rectangular channels with rib turbulators, *ASME J. Heat Transfer* **110,** 321–328 (1988).
10. S. Fann, W.-J.Yang and N. Li Zhang, Local heat transfer in a rotating serpentine passage with rib-roughened surface, *Int. J. Heat Mass Transfer* **37,** 217–228 (1994).
11. S. C. Lau, R. D. McMillin and J. C. Han, Turbulent heat transfer and friction in square channel with discrete rib turbulators, *ASME J. Turbomach.* **113,** 360–366 (1991).
12. S. C. Lau, R. T. Kukreja and R. D. McMillin, Turbulent heat transfer in a square channel with staggered discrete ribs, *J. Thermophys.* **6,** 171–173 (1992).
13. R. T. Kukreja, S. C. Lau and R. D. McMillin, Effects of length and configuration of transverse discrete ribs on heat transfer and friction for turbulent flow in a square channel, *Int. J. Turbo Jet Engnr* **9,** 301–310 (1992).
14. W. M. Kays and M. E. Crawford, *Convective Heat and Mass Transfer*. McGraw-Hill, New York (1966).
15. F. M. White, *Viscous Fluid Flow*. McGraw-Hill, New York (1974).